Journal of Materials Science and Chemical Engineering, 2015, 3, 69-77
Published Online December 2015 in SciRes. http://www.scirp.org/journal/msce
http://dx.doi.org/10.4236/msce.2015.312011

Production of CH_4 in a Low-Pressure CO_2/H_2 Discharge with Magnetic Field

Keisuke Arita, Satoru Iizuka

Department of Electrical Engineering, Graduate School of Engineering, Tohoku University, Sendai, Japan
Email: iizuka@ecei.tohoku.ac.jp

Received 4 November 2015; accepted 25 December 2015; published 28 December 2015

Abstract

Production of CH_4 has been established using a low-pressure square-pulse cross-field CO_2/H_2 discharge with magnetic field. The conversion rate from CO_2 to CH_4 was investigated by changing the discharge parameters such as applied power and discharge distance, together with magnetic field strength. Carbon dioxide was reduced by hydrogen. The discharge took place across the magnetic field inside a glass tube. Decomposition of CO_2 and CH_4 selectivity are found to be dependent on power density. Energy efficiency for methane production is increased in a narrow discharge. Preferable improvements of CO_2 decomposition, CH_4 selectivity, and energy efficiency were established.

Keywords

Carbon Dioxide, Methane, Pulse Discharge, Magnetic Field

1. Introduction

Carbon dioxide CO_2 is one of man-made greenhouse gases that are emitted by combustion of fossil fuels, such as coal, oil, and natural gas. Carbon dioxide is emitted from many power plants for generating electricity, power vehicles, heat homes, cook food and much more. However, fossil fuels are essentially a non-renewable energy source [1]. Therefore, the amount of fossil fuel reserves will be diminished in future by consumption and the cost of finding and extracting new underground resources will be much more expensive for everyday use [2] [3]. It might be also serious that CO_2 would cause global warming by absorbing and emitting radiation within the infrared range.

Therefore, the reduction of emission of carbon dioxide and the reduction of consumption of fossil fuels are crucial subject that must be settled urgently.

In order to suppress the emission of CO_2 into the environment from a power plant, for example, it might be

How to cite this paper: Arita, K. and Iizuka, S. (2015) Production of CH_4 in a Low-Pressure CO_2/H_2 Discharge with Magnetic Field. *Journal of Materials Science and Chemical Engineering*, **3**, 69-77. http://dx.doi.org/10.4236/msce.2015.312011

desirable that CO_2 is collected before exhausting and converted to methane, if any surplus renewable electric power exists. This means that surplus electric energy can be converted to chemical bonding energy of methane. That is, the surplus electric energy is stored as methane [4]-[6]. This method is superior to batteries, because the electric energy stored in batteries will be gradually lost by natural discharge. However, the energy stored in methane will be conserved for a long time without significant loss [7].

In order to reduce CO_2 with hydrogen various experiments were carried out by using discharge system [8]-[13]. In most cases, CO_2 was reduced by CH_4 to form syngas of CO and H_2 [14]-[20], because methane is also one of the greenhouse gases. Eliasson *et al.* investigated the production of CH_4 by a dielectric barrier discharge with H_2 in detail [8]. However, a new innovative method for improving CO_2 decomposition, CH_4 selectivity, and energy efficiency has been expected.

The purpose of this study is to investigate fundamental process of reduction of carbon dioxide to generate beneficial and reusable organic materials like methane by using low-pressure discharges [21] [22]. We here employed a low pressure discharge under the magnetic field. As well known, the discharge under atmospheric pressure was a very narrow streamer type. On the other hand, the discharge in low pressure was spatially spread and it was easy to obtain a non-equilibrium plasma, where the dissociation and decomposition effectively occurred by the electrons. In order to improve the reaction rate, the electron energy and density are quite important. Especially, in the low pressure, the magnetic field is useful to confine electrons to increase the electron density. The purpose of this experiment was to clarify the effect of discharge power on the formation of CH_4 by the reduction of CO_2 in low pressure discharge with hydrogen under the magnetic field.

2. Experimental Apparatus

Figure 1(a) shows a schematic of the experimental apparatus consisting of a coaxial cylindrical system [23]. Mixed gas of carbon dioxide and hydrogen was fed to the discharge chamber made of glass tube. The gas-mixing ratio and total flow rate were controlled by mass flow controllers, independently. Total pressure was adjusted by a needle valve and fixed at 200 Pa. Here, we employed a negative square-pulse voltage V_p with a pulse duration of 5 μs that was supplied to a small electrode. Repetition frequency of the square pulse was fixed at 1.25 kHz through the whole experiment. The gas passing through the discharge region was evacuated by a rotary pomp. Fourier transform infrared spectroscopy (FTIR) was employed to analyze the gas species before and after

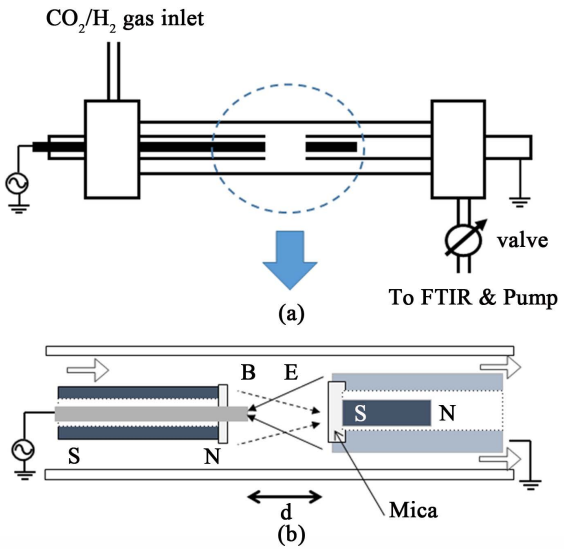

Figure 1. Schematic of the experimental setup. (a) Whole experimental system with inlet of mixed gas CO_2/H_2 and outlet to FTIR and rotary pomp. Pressure is adjusted by a needle valve. Details in a broken circle is shown in (b). A rod electrode is installed inside a pipe magnet (with polarity S and N) (left hand side), and a rod magnet is installed inside a grounded stainless pipe electrode (right hand side). *d* denotes electrode distance (=2 - 3 mm). Gas flow direction is indicated by white arrows. Directions of crossed magnetic and electric fields denoted by *B* and *E* in the discharge region are indicated by dotted and solid arrows, respectively.

the discharge [21] [22]. For the measurement of small amounts of gas species, the sampled gas was introduced into FTIR with a gas cell with multiple laser reflection system, where precise absolute values of each gas species were possible to measure by comparing with typical FTIR signal database.

In order to proceed a discharge under the magnetic field, two kinds of permanent magnets were employed as shown in **Figure 1(b)**. One was a pipe magnet (17 mm long, 4 mm inner diameter, and 9 mm outer diameter) made of samarium cobalt, the magnetic strength of which was 0.4T at the end surface. The other one was a rod magnet (27 mm long, 4 mm diameter) made of samarium cobalt, the magnetic strength of which was also 0.4T at the end surface. Inside the pipe magnet a powered electrode of 2 mm in diameter was inserted for the discharge from the left-hand side as shown in **Figure 1(b)**. The grounded electrode was a stainless pipe (50 mm long, 6 mm inner diameter, and 8 mm outer diameter), inside of which the rod magnet was installed. In order to avoid direct contact between the plasma and the magnets, thin mica plate of 0.5 mm thick was attached to the end surface of the magnets. The tip of the powered electrode protruded 1 mm from the mica plate. The entire electrode system was installed inside the glass tube of 10 mm in inner diameter and 12 mm in outer diameter. Gas flow direction was indicated by thick white arrows in **Figure 1(b)**.

Since the magnetic field and the electric field supplied by the magnets and powered electrode, respectively, intersect with an oblique angle each other, as shown in **Figure 1(b)**, a cross field discharge, *i.e.*, a glow discharge with a perpendicular component of magnetic field, can be realized. The discharge under the magnetic field has an advantage for increasing the electron density in a core plasma region and reducing the electron diffusion across the magnetic field toward downstream region. Owing to the electron density increase, dissociation of CO_2 and H_2 will be enhanced. On the other hand, suppression of electron diffusion toward downstream region will reduce re-decomposition of CH_4 by electrons. As a result, an enhancement of CH_4 yield is expected.

3. Experimental Results and Discussions

3.1. Experimental Conditions

The degree of electron magnetization was evaluated from $\omega_{ce}\tau_{cn} \sim 7.5$ for hydrogen at 200 Pa. Here, ω_{ce} is electron cyclotron angular frequency at the magnetic field of $B = 0.4$ T and τ_{cn} is collision time of electrons with neutral hydrogen. Since $\omega_{ce}\tau_{cn}$ was much larger than 1, the electrons were sufficiently magnetized.

Variations of the magnetic field strength supplied by the pipe magnet and the rod magnet along the center axis are plotted in **Figure 2** by sold and dotted curves, respectively, as a function of the distance from the surface of the powered electrode. Actual magnetic field strength at the position between the electrodes can be obtained by a summation of both components of magnetic field. Therefore, the magnetic field of 0.45 - 0.55 T was applied in the discharge space. From this configuration we could investigate hydrogenation of CO_2 to CH_4 under magnetic field.

The results were evaluated by the following quantities.

(i) CO_2 decomposition ratio α (%):

$$\alpha = 1 - \frac{[CO_2]_1}{[CO_2]_0} \tag{1}$$

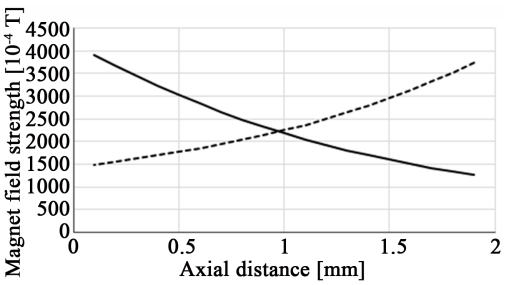

Figure 2. Variations of magnetic field strength, supplied by a pipe magnet (solid curve) and a rod magnet (dotted curve), along the center axis of a glass tube in the region indicated by a double-headed arrow in **Figure 1**. The distance was counted from the surface of powered electrode. The electrode distance was 2 mm.

(ii) CH_4 selectivity β (%):

$$\beta = \frac{[CH_4]}{[\text{all carbon species produced}]} \tag{2}$$

(iii) Energy efficiency γ (L/kWh) for CH_4 production:

$$\gamma = \frac{[CH_4 \text{ produced in litter}]}{\text{electric energy consumed by the discharge}} \tag{3}$$

Here, [a] denotes amount of a, and suffix 0 and 1 correspond to the values before and after the discharge, respectively. These quantities show how much carbon in CO_2 has been converted to methane. γ is also an important factor to realize a suitable commercial system for producing methane in high efficiency. Discharge power was obtained by a time averaged value of $V(t)I(t)$ supplied from the pulse generator, where $V(t)$ and $I(t)$ were applied voltage and discharge current at time t, respectively. Here, 1 L/kWh corresponds to 44.6 mmol/kWh (=0.71 g(CH_4)/kWh). Energy efficiency can be also expressed by $\gamma = \alpha\beta\Gamma/100P_{in}$, where Γ is input partial flow rate of CO_2 and P_{in} is input electric power for the discharge.

Gas species measured by FTIR showed that main carbon products were CH_4 and CO through the whole experiment. Here, CO might come from the following dissociation reaction by electron impact collisions; $e + CO_2 \rightarrow CO + O$. Hydrocarbon species was only CH_4, and the other COH_2 and CH_3OH were not detected. We could not detect other organic materials such as ethane, ethylene, and acetylene. But, the production of steam H_2O was detected. Therefore, it was shown that methane was actually only a hydrocarbon produced from CO_2. Therefore, in this case, methane selectivity β could be simply expressed by $\beta = [CH_4]/([CH_4] + [CO])$. Through the experiment we fixed pulse repetition frequency of applied pulse voltage at 1.25 kHz. Flow rate of CO_2 was also fixed at 1 sccm (standard cubic centimetres).

3.2. H_2 Flow Rate Dependence

Dependencies of CO_2 decomposition ratio α, CH_4 selectivity β, and energy efficiency γ on H_2 flow rate were briefly reported in Ref. [23] with and without magnetic field. The discharge power was set at 30 W. When the magnetic field was introduced, the maximum β of 27% was obtained at H_2 = 10 sccm. This value was higher than that of about 16% in the case without magnetic field. It was found that γ in the case with magnetic field raised almost 3 times as much as that in the case without magnetic field. The maximum value of γ attained to about 0.46 L/kWh when H_2 flow rate was about 10 sccm.

In our system α was not much changed by the hydrogen flow rate. However, β has a strong dependence on H_2 flow rate in the regime below 10 sccm [23]. The maximum of β attained to about 27% at H_2 = 10 sccm when the cross field discharge was employed. In the lower H_2 flow rate regime the reaction was determined by amount of H_2 supplied. The production of CH_4 was increased with an increase in H_2 flow rate, according to the following reaction.

$$CO_2 + 4H_2 = CH_4 + 2H_2O(\text{gas}) \tag{4}$$

Here, taking account of a simultaneous production of CO it was reasonable that optimum amount of H_2 for CH_4 production exceeded stoichiometry value of 4 sccm, *i.e.*, CO_2:H_2 = 1:4 as in reaction (4). When H_2 flow rate was much more increased, transit time of H_2 gas flow within the discharge region was decreased, which might result in a decrease in CH_4 production.

3.3. Input Power Dependence

In our system, permanent magnets were directly attached to the electrode via a thin mica insulator sheet of 0.5 mm thick, in order to avoid heat damage and to keep electrical insulation. Therefore, a change of the electrode distance d between the powered electrode and the grounded pipe electrode also brought about a change of the strength of magnetic field B in the discharge region. That is, when d was changed from 2 mm to 3 mm, the strength of magnetic field at the middle point on the center axis between the electrodes was varied from 0.45 T [= 0.225 T (dotted curve) + 0.225 T (solid curve)] to 0.335 T [= 0.175 T (dotted curve) + 0.16 T (solid curve)] (see **Figure 2**).

Input power P_{in} dependencies of α were plotted in **Figure 3** with the electrode distance d as a parameter. Here, flow rate ratio was kept at CO_2:H_2 = 1 sccm:4 sccm. With increasing input power, CO_2 decomposition ratio β increased and attained to 25% at P_{in} = 40 W when d = 2 mm. Then, the decomposition ratio β was gradually saturated and approached to 35% when P_{in} was further increased to 160 W. One of the reasons for this saturation was an input power loss by a heating of the electrodes, rather than a production of plasma. It was also noted that a small gap distance between the electrodes was effective for the decomposition of CO_2. This might be due to an increase of the electric field for the plasma production and a resultant increase of input power density for CO_2 decomposition, when the electrode distance d was changed from 3 mm to 2 mm.

Similar dependency was observed for CH_4 selectivity β as shown in **Figure 4**. In the case of d = 2 mm, β increased almost in proportion to input power in the range P_{in} < 30 W. We got β = 30% at P_{in} = 30 W. However, the increment rate of β was reduced in the range P_{in} > 30 W. Even in this case, however, β attained to 35% when P_{in} = 130 W. It was also found that the input power for getting the same value of β was reduced by decreasing d from 3 mm to 2 mm. We got β = 30% when P_{in} was increased up to 50 W.

Production rate of methane can be obtained from the product $\alpha\beta\Gamma/100$. Here, Γ (=1 sccm) is the initial flow rate of CO_2. **Figure 5** shows the production ratio of $CH_4$from CO_2as a function of input power with d as a parameter. Vertical axis also shows how much percent of CO_2 is converted to CH_4via a reaction with H_2. With an increase in input power P_{in}, the production of CH_4 was increased almost in proportion to input power. However, CH_4production was saturated above 50 W, and finally about 15% of CO_2 was converted to CH_4 at P_{in} = 160 W

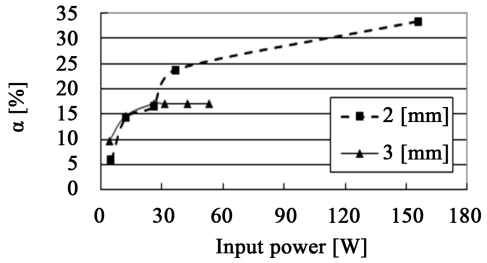

Figure 3. Variation of CO_2 decomposition ratio α as a function of input electric power with electrode distance d as a parameter in the case with magnetic field. Flow rate ratio is CO_2:H_2 = 1 sccm:4 sccm.

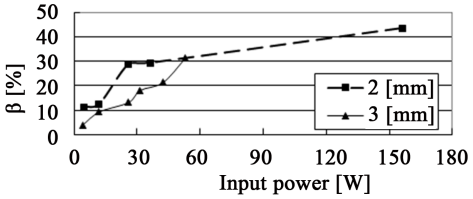

Figure 4. Variation of CH_4 selectivity β as a function of input electric power with d as a parameter in the case with permanent magnets. Flow rate ratio is CO_2:H_2 = 1 sccm:4 sccm.

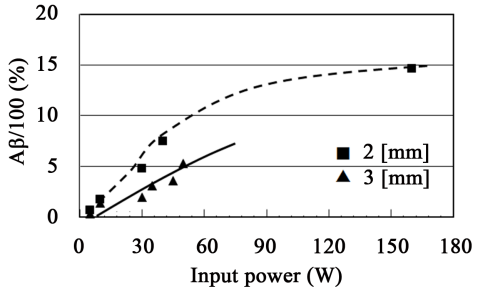

Figure 5. Production ratio of CH_4 from CO_2 as a function of input power with d as a parameter in the case with permanent magnets. Vertical axis shows how much percent of CO_2 is converted to CH_4. Flow rate ratio was CO_2:H_2 = 1 sccm:4 sccm.

in the case of d = 2 mm. Production efficiency in the case of d = 2 cm is roughly two times as much as that in the case of d = 3 cm.

Finally, power dependence of energy efficiency γ was plotted in **Figure 6** with d as a parameter. We got maximum γ of 0.53 L/kWh when P_{in} = 30 W and d = 2 mm. Although β and β increased with input power, γ was conversely reduced to about a half at P_{in} = 160 W. Therefore, the total energy efficiency was fairly reduced in the high power regime. It was noted that γ became low in the overall power regime when d = 3 mm, compared to the case of d = 2 mm. This might be due to a decrease of input power density for the plasma production as mentioned above.

The results shown in **Figure 3** and **Figure 4** were replotted in **Figure 7(a)** and **Figure 7(b)**, respectively, as a function of power density (W/mm^3) with the electrode distance d as a parameter. Here, power density was obtained from input power (W) divided by the discharge space volume (mm^3). The decomposition ratio α seemed to be simply dependent on the input power density (W/mm^3), rather than d, as shown in **Figure 7(a)**. The value α increased with an increase in power density and finally reached 25% at 0.2 W/mm^3. Then, β was gradually saturated in the higher power density range (>0.2 W/mm^3). Similar dependence was also found for the CH_4 selectivity β. The dependence of β on power density seemed to be nearly independent of d, but dependent on power density as shown in **Figure 7(b)**. The value of β was abruptly increased with an increase in input power density below 0.2 W/mm^3, and finally saturated around 30% at about 0.2 W/mm^3. Then, β gradually increased in the higher power density regime (>0.2 W/mm^3).

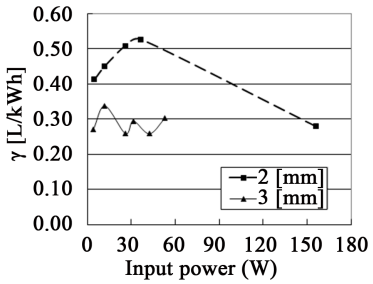

Figure 6. Variation of energy efficiency γ as a function of input electric power with d as a parameter in the case with permanent magnets. Flow rate ratio was CO_2:H_2 = 1 sccm:4 sccm.

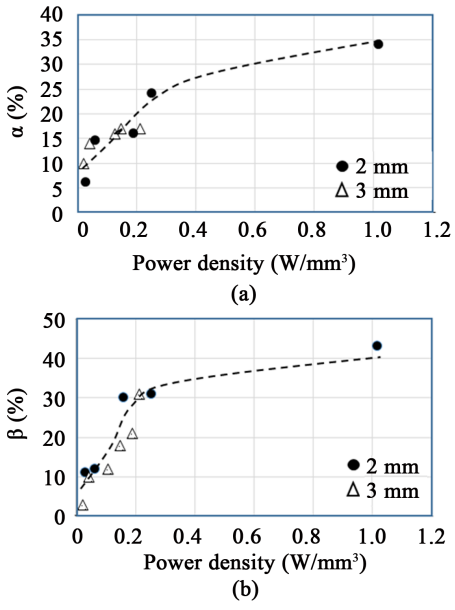

Figure 7. Variation of CO_2 decomposition ratio α and CH_4 selectivity β as a function of input electric power density with d as a parameter in the case with permanent magnets. Flow rate ratio was CO_2:H_2 = 1 sccm:4 sccm.

4. Discussion

Discharge within a very narrow gap of 2 mm in the presence of magnetic field was quite effective for conversion from CO_2 to methane. Under the magnetic field, electrons are magnetized and confined for a long time in the discharge. Owing to these electrons, mixed gas of CO_2 and H_2 was decomposed in the discharge and finally CH_4 was produced in the downstream region through a recombination of decomposed radicals. The decomposition ratio was expectedly increased in a plasma with magnetic field.

Figure 8 schematically shows a model for CH_4 production in the cases (a) without and (b) with the magnetic field. As shown in **Figure 8(a)**, when no magnetic field is applied, the electrons produced between the electrodes diffuse toward the downstream region as shown by thick arrows, with radicals CO^*, H_2^*, and H^*, which are mainly produced by electron impact collisions in a core plasma, *i.e.*, $e + CO_2 \rightarrow CO^* + O^*$ and $e + H_2 \rightarrow H_2^* \rightarrow H^* + H^*$. Eventually, these radicals react with each other to produce CH_4 in the downstream region. It should be noted that, during this synthesis process, however, CH_4 produced would be simultaneously re-decomposed by the electrons through the following electron impact dissociation collisions, *i.e.*, $e + CH_4 \rightarrow CH_2^* + H_2^*$. Then, total amount of CH_4 production would be suppressed during the diffusion in the presence of elections as in a core plasma region between the electrodes. Therefore, CH_4 selectivity β would be reduced.

On the other hand, when the magnetic field is introduced, magnetized electrons are suppressed to diffuse across the magnetic field toward the downstream recombination reaction region. On the other hand, neutral radicals, which are not magnetized, are able to diffuse toward the downstream region as shown by white arrows in **Figure 8(b)**. Then, CH_4 synthesis proceeds among those radicals in such electron-suppressed downstream space, where simultaneous re-decomposition of CH_4 by electron impact dissociation collisions were reduced. Then, CH_4 selectivity β would be improved.

Further, since the magnetic field can confine the electrons, electron density in the core plasma region increases. Then, CO_2 decomposition ratio β is also increased by the following dissociative collisions with electrons, *i.e.*, $e + CO_2 \rightarrow CO^* + O^*$. As a result of the increases in α and β, energy efficiency γ could be markedly increased in the case with the magnetic field, as shown in **Figure 6**.

As shown in **Figure 7**, α and β are a function of power density, increasing with power density. This result can explain the results in **Figure 6**. That is, when the input power is fixed, the power density in the case of d = 2 mm can be higher than that of d = 3 mm. Therefore, both β and β in the case of d = 2 mm would be higher than those in the case of d = 3 mm at fixed input power. Therefore, since $\gamma \sim \beta$, a large γ can be obtained when d = 2 mm. Actually, energy efficiency γ attained to 0.53 L/kWh, which was rather higher than those of the previous magnetic-field free experiments [8] [9]. The use of magnetic field is quite effective for a higher rate conversion of CO_2 to CH_4.

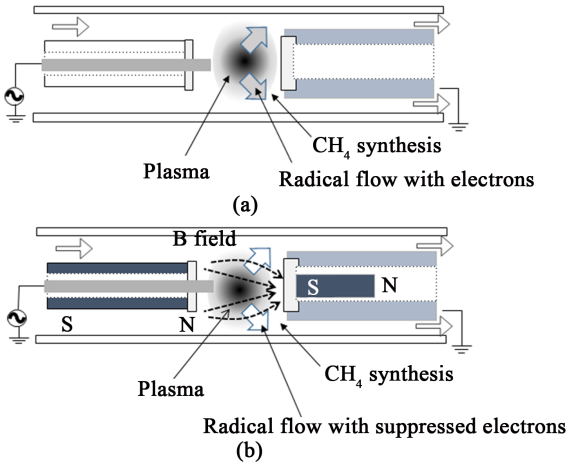

Figure 8. A model of CH_4 synthesis in (a) absence and (b) presence of magnetic field (dotted line). In (a), both electrons and neutral radicals (CO^*, H_2^*) diffuse toward downstream recombination region, where CH_4 is formed with an effect of re-decomposition by electrons. In (b), diffusion of magnetized electrons across the magnetic field is suppressed. CH_4 synthesis proceeds with less effect of re-decomposition by electrons.

The energy efficiency γ described above did not include the energy for generating H_2 from the water, for example. Electrolysis is a promising option for hydrogen production using renewable resources. Industrial electrolyzer has a nominal hydrogen production efficiency of around 73% [24]. Further, a maximum efficiency value of 96% was reported for the case of low carbon steel electrodes, which was much higher than 73%, the average efficiency of common commercial and industrial electrolyzers [25]. Here, we concentrated only on the energy efficiency for the production of CH_4 from CO_2 with a use of given H_2 and CO_2.

Finally, we discuss a carbon balance. As mentioned above, the materials containing carbon, produced by the discharge, were simply CH_4 and CO. Methanol was scarcely produced. The other carbon materials such as COH_2 and C_2 hydrocarbons like ethane, ethylene, and acetylene were not detected. Carbon film deposition was also not observed in a lower power regime (<30 W) when $[H_2]/[CO_2] \gg 1$. This would be due to the fact that carbon atom might be immediately either oxidised by oxygen or reduced by hydrogen when carbon atoms were produced in the discharge. The resultant carbon balance was simply expressed as follows:

$$\alpha[\mathrm{CO_2}] \sim \alpha\beta[\mathrm{CH_4}] + \alpha(1-\beta)[\mathrm{CO}]$$

As described above, in our experiment, CO_2 and H_2 were decomposed to form CO^*, H_2^* and H^* by electrons in the plasma. Then, CO^* was reduced by H_2^* and H^*, and finally CH_4 was produced. This process was quite similar to Sabatier reaction [26], where CO_2 was dissociated to $CO^* \rightarrow C^* + O^*$ on a heated Ni surface. Then, H_2 reacted with C^* and O^* on Ni surface to generate CH_4 [27] [28]. In our case, the electrons in the plasma played a similar role as a catalysis effect of Ni.

It should be also noted that γ in our discharge system was much higher than that of conventional magnetic-field free discharges. The energy efficiency in the case of high-pressure dielectric-barrier discharge (DBD) was reported to be 0.06 L/kWh, where β = 12.4%, β = 3.2% for the total flow rate of Γ = 500 sccm (CO_2:H_2 = 1:3) and input power of 500 W [8]. For a low pressure microwave discharge, γ = 0.027 L/kWh was reported with β = 81% and β = 1.2% at input power of 3 kW [9]. Therefore, energy efficiency in our case was about 20 times as much as that in the low-pressure microwave case.

5. Conclusion

Methane was produced from carbon dioxide in a low-pressure square-pulse cross-field discharge with hydrogen. Methane was only organic species produced from CO_2. Only CO was detected as non-organic by-product. We found that the decomposition ratio β of CO_2, methane selectivity β, and energy efficiency γ in a short electrode distance under the magnetic field were superior to those of the magnetic-field free cases. We obtained β = 25%, β = 30%, and γ = 0.53 L/kWh under optimized condition at flow rate ratio of CO_2:H_2 = 1:4, electrode distance of d = 2 mm, and input power of P_{in} = 30 W under the magnetic field of 0.45 T. Therefore, the discharge in a small volume with magnetic field was effective for an efficient production of CH_4 from CO_2 in a low pressure CO_2/H_2 discharge plasma.

References

[1] BP: World Reserves of Fossil Fuels. http://jp.knoema.com/smsfgud/bp-world-reserves-of-fossil-fuels

[2] Gore, A. The End of Fossil Fuels. https://www.ecotricity.co.uk/our-green-energy/energy-independence/the-end-of-fossil-fuels

[3] Shafiee, S. (2008) An Overview of Fossil Fuel Reserve Depletion Time. 31*st IAEE International Conference*, Istanbul, 18-20 June 2008. http://espace.library.uq.edu.au/view/UQ:197790

[4] Struckmann, L.K.R., Pesched, A., Rauschenbach, R.H. and Sundmacher, K. (2010) Assessment of Methanol Synthesis Utilizing Exhaust CO_2 for Chemical Storage of Electrical Energy. *Industrial & Engineering Chemistry Research*, **49**, 11073. http://dx.doi.org/10.1021/ie100508w

[5] Lunsford, J.H. (2000) Catalytic Conversion of Methane to More Useful Chemicals and Fuels: A Challenge for the 21st Century. *Catalysis Today*, **63**, 165. http://dx.doi.org/10.1016/S0920-5861(00)00456-9

[6] McDonough, W., Braungart, M., Anastas, P. and Zimmerman, J. (2003) Applying the Principles of Green Engineering to Cradle-to-Cradle Design. *Environmental Science & Technology*, **37**, 434A. http://dx.doi.org/10.1021/es0326322

[7] Schaaf, T., Grunig, J., Schuster, M.R., Rothenfluh, T. and Orth, A. (2014) Methanation of CO2—Storage of Renewable Energy in a Gas Distribution System. *Energy, Sustainability and Society*, **4**, 29.

[8] Eliasson, B., Kogelschatz, U., Xue, B. and Zhou, L.M. (1998) Hydrogenation of Carbon Dioxide to Methanol with a

Discharge-Activated Catalyst. *Industrial & Engineering Chemistry Research*, **37**, 3350. http://dx.doi.org/10.1021/ie9709401

[9] Gouyard, V., Ttibouet, J. and Duperyrat, C.B. (2009) Influence of the Plasma Power Supply Nature on the Plasma-Catalyst Synergism for the Carbon Dioxide Reforming of Methane. *IEEE Transactions on Plasma Science*, **37**, 2342. http://dx.doi.org/10.1109/TPS.2009.2033695

[10] Larkin, D.W., Lobban, L.L. and Mallinson, R.G. (2001) Production of Organic Oxygenates in the Partial Oxidation of Methane in a Silent Electric Discharge Reactor. *Industrial & Engineering Chemistry Research*, **40**, 1594. http://dx.doi.org/10.1021/ie000527k

[11] Mei, D., Zhu, X., He, Y.K., Yan, J.D. and Tu, X. (2015) Plasma-Assisted Conversion of CO_2 in a Dielectric Barrier Discharge Reactor: Understanding the Effect of Packing Materials. *Plasma Sources Science and Technology*, **24**, Article ID: 015011. http://dx.doi.org/10.1088/0963-0252/24/1/015011

[12] Hoeben, W.F.L.M., Boekhoven, W., Beckers, F.J.C.M., Van Heesch, E.J.M. and Pemen, A.J.M. (2014) Partial Oxidation of Methane by Pulsed Corona Discharges. *Journal of Physics D*: *Applied Physics*, **47**, Article ID: 355202. http://dx.doi.org/10.1088/0022-3727/47/35/355202

[13] Spencer, L.F. and Gallimore, A.D. (2011) Efficiency of CO_2 Dissociation in a Radio-Frequency Discharge. *Plasma Chemistry and Plasma Processing*, **31**, 79-89. http://dx.doi.org/10.1007/s11090-010-9273-0

[14] Ross, J.R.H. (2005) Natural Gas Reforming and CO_2 Mitigation. *Catalysis Today*, **100**, 151-158. http://dx.doi.org/10.1016/j.cattod.2005.03.044

[15] Mikkelsen, M., Jorgensen, M. and Krebs, F.C. (2010) The Teraton Challenge. A Review of Fixation and Transformation of Carbon Dioxide. *Energy & Environmental Science*, **3**, 43-81. http://dx.doi.org/10.1039/B912904A

[16] Snoeckx, R., Aerts, R., Tu, X. and Bogaerts, A. (2013) Plasma-Based Dry Reforming: A Computational Study Ranging from the Nanoseconds to Seconds Time Scale. *The Journal of Physical Chemistry C*, **117**, 4957-4970. http://dx.doi.org/10.1021/jp311912b

[17] Dorai, R., Hassouni, H. and Kushner, M.J. (2000) Interaction between Soot Particles and NOX during Dielectric Barrier Discharge Plasma Remediation of Simulated Diesel Exhaust. *Journal of Applied Physics*, **88**, 6060-6071. http://dx.doi.org/10.1063/1.1320004

[18] Tao, X., Bai, M., Li, X., Long, H., Shaung, S., Yin, Y. and Dai, X. (2011) CH_4-CO_2 Reforming by Plasma—Challenges and Opportunities. *Progress in Energy and Combustion Science*, **37**, 113-124. http://dx.doi.org/10.1016/j.pecs.2010.05.001

[19] Xu, C. and Tu, X. (2013) Plasma-Assisted Methane Conversion in an Atmospheric Pressure Dielectric Barrier Discharge Reactor. *Journal of Energy Chemistry*, **22**, 420-425. http://dx.doi.org/10.1016/S2095-4956(13)60055-8

[20] Aerts, R., Somers, W. and Bogaerts, A. (2015) Carbon Dioxide Splitting in a Dielectric Barrier Discharge Plasma: A Combined Experimental and Computational Study. *ChemSusChem*, **8**, 702-716. http://dx.doi.org/10.1002/cssc.201402818

[21] Kano, M., Satoh, G. and Iizuka, S. (2012) Reforming of Carbon Dioxide to Methane and Methanol by Electric Impulse Low-Pressure Discharge with Hydrogen. *Plasma Chemistry and Plasma Processing*, **32**, 177-185. http://dx.doi.org/10.1007/s11090-011-9333-0

[22] Tsuchiya, T. and Iizuka, S. (2013) Conversion of Methane to Methanol by a Low-Pressure Steam Plasma. *Journal of Environmental Engineering and Technology*, **2**, 35-39.

[23] Arita, K. and Iizuka, S. (2015) Hydrogenation of CO_2 to CH_4 Using a Low-Pressure Cross-Field Pulse Discharge with Hydrogen. *Proceedings of the* 22*nd International Symposium on Plasma Chemistry*, Antwerp, 5-10 July 2015.

[24] Mazloomi, K., Sulaiman, N. and Moayedi, H. (2012) Electrical Efficiency of Electrolytic Hydrogen Production. *International Journal of Electrochemical Science*, **7**, 3314-3326.

[25] Wei, Z.D., Ji, M.B., Chen, S.G., Liu, Y., Sun, C.X., Yin, G.Z., Shen, P.K. and Chan, S.H. (2007) Water Electrolysis on Carbon Electrodes Enhanced by Surfactant. *Electrochimica Acta*, **52**, 3323-3329. http://dx.doi.org/10.1016/j.electacta.2006.10.011

[26] Schaaf, T., Grunig, J., Schuster, M.R., Rothenfluh, T. and Orth, A. (2014) Methanation of CO_2—Storage of Renewable Energy in a Gas Distribution System. *Energy, Sustainability and Society*, **4**, 29.

[27] Fujita, S., Teruuma, H., Nakamura, M. and Takezawa, N. (1991) Mechanisms of Methanation of Carbon Monoxide and Carbon Dioxide over Nickel. *Industrial & Engineering Chemistry Research*, **30**, 1146-1151. http://dx.doi.org/10.1021/ie00054a012

[28] Hoekman, S.K., Broch, A., Robbins, C. and Purcell, R. (2010) CO_2 Recycling by Reaction with Renewably-Generated Hydrogen. *International Journal of Greenhouse Gas Control*, **4**, 44-50. http://dx.doi.org/10.1016/j.ijggc.2009.09.012